Polymer 51 (2010) 5771–5779

Contents lists available at ScienceDirect

Polymer

journal homepage: www.elsevier.com/locate/polymer

Cavitation during tensile drawing of annealed high density polyethylene

Andrzej Pawlak*, Andrzej Galeski

Center of Molecular and Macromolecular Studies, Polish Academy of Sciences, Sienkiewicza 112, 90-363 Lodz, Poland

ARTICLE INFO

Article history:
Received 5 May 2010
Received in revised form
30 September 2010
Accepted 1 October 2010
Available online 12 October 2010

Keywords:
Cavitation
Plastic deformation
Polyethylene

ABSTRACT

Annealing of semicrystalline polymers usually leads to refinement and thickening of crystals. It appears that also cavitation is affected during tensile drawing. In the uniaxially drawn high density polyethylene massive cavitation was detected by X-ray scattering in the samples previously annealed at 125 °C. The number of voids depends on the annealing time, while their size and orientation depends on the local strain. Cavitation resulted in 30% increase in volume for the annealed samples, strained to 4–5. Cavitation and volume increase were not observed for small and intermediate strains if polyethylene samples were not annealed. The decrease in the drawing rate results in the reduction of cavitation and void stability – at the low strain rate voids were detected during tensile drawing, though they disappeared after unloading the sample.

1. Introduction

The deformation modes of a semicrystalline polymer involve both amorphous and crystalline components [1,2]. The formation of cavities was observed in the amorphous phase of many polymers during tensile deformation. Cavitation appears at or around the yield point [3–7]. One can trace the progress in understanding of the voiding mechanism in the literature published during last 10 years [8–17]. Our studies have shown that some polymers do not cavitate, while others cavitate under certain deformation conditions [10,11]. The reason for such behavior is competition between two mechanisms of deformation of a stressed polymer near the yield point – initiation of plastic deformation of crystalline elements, lamellae, usually by crystallographic slips, and generation of numerous voids in the stretched amorphous phase between crystalline lamellae [10]. Therefore, the way in which the deformation proceeds depends on the relation between the resistance of the amorphous phase to cavitation and the resistance of polymer crystals to plastic deformation. In typical crystallizing polymers, such as high density polyethylene or polypropylene, cavitation is usually first observed, however its occurrence depends in particular on the morphology of the material and the deformation conditions [11].

Annealing increases perfection of crystals and their thickness [1]. Some observations indicate that a non-cavitating sample may cavitate after annealing [16]. The main goal of our current work was to determine such transition in the annealed high density polyethylene and the accompanying changes in shape, size and concentration of cavities with an increase in the annealing time at certain stages of deformation. The influence of the strain rate was also studied. Our hypothesis is that there is a limiting drawing rate below which a non-cavitational mechanism of deformation is favored.

Usually cavities are detected by small angle X-ray scattering or by a visual observation of stress whitening [5,6,8]. It was demonstrated that the measurement of volume change may also be a method of detecting the presence of cavities in the material [14,18,19]. Determination of relations between the mechanical properties and the changes in the internal morphology by X-ray diffraction has recently become easier, since the sources of powerful synchrotron radiation are more accessible. Results of *in situ* small- (SAXS) and wide-angle X-ray scattering (WAXS) measurements for many polymers were described in the past [20–26]. However, our paper is one of the first to combine *in situ* measurements of X-ray scattering, X-ray diffraction, mechanical properties and volume change.

The studies of polyethylene's deformation have shown that cavitation may be accompanied by other processes. Butler et al. [16] examined quenched and annealed samples of PE and detected cavitation at yield at the time when low intensity martensitic transformation occurred. However, martensitic transition should not be associated with cavitation because it was also observed in compression of polyethylene, where voids were not formed [1,17]. The phenomenon that occurs most frequently around yielding simultaneously with cavitation is fragmentation of lamellae [16].

SAXS patterns indicate that voids in deformed polymers are initially elongated perpendicularly to the direction of deformation, but at a certain strain the change in shape occurs and in highly deformed polymers voids are elongated along the direction of

* Corresponding author. Tel.: +48 42 6803223; fax: +48 42 6847126.
E-mail address: apawlak@bilbo.cbmm.lodz.pl (A. Pawlak).

0032-3861/$ – see front matter © 2010 Elsevier Ltd. All rights reserved.
doi:10.1016/j.polymer.2010.10.003

deformation [10,11,13]. When lamellar polymer crystals are transformed into fibrillar structure, the voids often become very large and may join together.

The results of studies of cavitation during tensile deformation of HDPE samples quenched and annealed for different periods of time prior to tensile drawing are discussed below. The drawing rates, selected from a wide range, were applied in order to determine its limiting value, below which cavitation does not occur in the annealed samples.

2. Experimental

High density polyethylene BASF Lupolen 6021D (M_w 1.8 $\times$ 10^5, $M_w/M_n = 7.2$, density 0.960 g/cm^3, MFI = 0.26 g/10 min at 2.16 kg, 190 °C) was selected for studies. Samples for experiments were prepared by compression molding at the temperature of 190 °C, followed by rapid cooling in water with ice and 1 mm thick sheets were produced. Some of the sheets were annealed inside a heating chamber at the temperature of 125 °C, the annealing time being 1, 3 or 6 h; the others were used as a reference material. Dog-bone tensile samples were then cut out from the sheets, according to ASTM D 638 Type V standard.

Mechanical tensile properties of HDPE were studied at room temperature using Instron 5582 mechanical testing machine. Standard engineering drawing rate was 8.3 $\times$ 10^{-4} s^{-1} (i.e. 5%/min), however some samples were deformed at lower rates: 6.7 $\times$ 10^{-5} s^{-1} (0.4%/min) and 2.5 $\times$ 10^{-5} s^{-1} (i.e. 0.15%/min). We limited deformation to engineering strain of 75–100%, much below the strain to break. The actual shape of a sample during deformation was recorded by a "Minolta Dimage" digital camera. A mirror was applied for the simultaneous recording of thickness – the third dimension of a sample. The actual cross-section was calculated from the measured dimensions of the sample. In order to measure local deformation, black ink marks were placed on the surface of the sample at the distances of 1 mm. The local strain was determined as a change in distance between marks, $l - l_o$, divided by the original distance l_o. The volume strain was calculated as a change in volume, $\Delta V = V - V_o$, divided by the initial volume, V_o, measured in the most deformed part of the sample. The accuracy of volume measurements is usually estimated at the level of 1–2%. Moreover, the individual differences between samples were observed and averaged.

The small angle X-ray scattering (SAXS) was performed in a synchrotron beamline A2 at Hasylab (Desy) in Hamburg, the aim being precise detection of cavitation. X-ray wavelength from synchrotron source was 0.15 nm and the distance from the sample to the detector was 2.6 m. Tensile *in situ* observations of void formation were possible thanks to a custom-made tensile testing machine fitted to the beamline. Signals from a load cell and from a transducer measuring elongation were recorded during the experiment. It was possible to observe the sample and the position of the X-ray beam by a TV-camera and to record the consecutive video frames. The beam was positioned in the region of the smallest cross-section of the sample. The variation of the cross-section area in our samples did not exceed 1%. In more than 50% cases a neck was formed in the area where the beam was positioned. Such examples are discussed further. The size of the beam was around 1 mm along the direction of deformation, therefore the neck zone was included within the beam spot shortly after yielding. The deformation was performed at the selected rates of 8.3 $\times$ 10^{-4} s^{-1}, 6.7 $\times$ 10^{-5} s^{-1} and 2.5 $\times$ 10^{-5} s^{-1}, the same as used in the tensile test described above. The details of the experimental synchrotron procedure are described in the paper by Stribeck [21]. SAXS patterns were also applied for determination of a long period of the structure of polyethylene samples. The position of the maximum on the curve I^*s^2 vs. s, where I is the intensity of scattering and s is the scattering vector were used for calculations. The thickness of lamellae was determined using a correlation function method [27,28].

In order to determine the size of cavities, the method described by Yamashita et al. has been adopted [29]. The function of ln(I) vs. s^2, where I is the intensity of scattering and s is the scattering vector provided the basis for calculation of the radius of gyration (R_g). The radius of gyration depends on the dimensions of scattering objects. Since the dependence $\ln(I) = f(s^2)$ is not linear for deformed HDPE, the range of the scattering vector was divided into two parts, in which the dependence $\ln(I) = f(s^2)$ is approximately linear. Each of the parts represent different population of cavities, differing in size. The contribution of each group of voids to the total scattering was determined and next the radii of gyration were calculated, starting from the smallest voids.

Wide-angle X-ray scattering (WAXS) camera was used for the observation of lamellar orientation. A source of CuK_α radiation was used. Two-dimensional scattering images were recorded with a camera equipped with a Kodak imaging plate. Stretching of the sample was interrupted at the selected strain and the sample was fixed in a special frame which preserved the state of strain. The frame with the sample was then placed in a holder of WAXS apparatus. A typical time of acquisition was 7 min. For some HDPE samples WAXS patterns were recorded after relaxation of mechanical stress with the aim of detecting possible changes in the diffraction patterns. We supposed that the lack of scattering from monoclinic form of HDPE may sometimes result from relaxation of the deformed sample before WAXS studies.

The degree of crystallinity, melting temperature, length of crystalline stem and lamellar thickness were determined from the heat of melting and the peak of melting temperature [30] using a DSC 2920 differential scanning calorimeter (TA Instruments). The inclination of crystalline stems by 35° to the normal of the lamellar surface [31] was taken into account in the calculations of lamellar thickness L.

Resistance to degradation of initial and annealed samples was estimated by determination of Oxidation Induction Time, performed according to EN 728:1997 E standard.

3. Results and discussion

The compression molding followed by rapid cooling of molten polyethylene in iced water gave us a material with small, imperfect crystals and with a relatively low degree of crystallinity. Annealing in the controlled thermal conditions was a way to improve perfection of crystals, increase their thickness and total crystallinity. The crystalline properties of annealed HDPE are presented in Table 1, where DSC and SAXS data have been collected. Table 1 shows that nearly 10% increase in crystallinity is observed after 1 h of annealing. Longer times favor further, though less rapid, increase. The maximum degree of crystallinity, 81%, was obtained when the polymer was annealed for 6 h. The absolute values of crystallinity depend on the values of parameters taken into calculation, such as heat of fusion [32], however a systematic error seems to be insignificant when the same values are taken for a series of compared samples, as was in our case.

The second important parameter characterizing a polymer, mean thickness of lamellae, also increases with the annealing time. Initial, 20 nm thick crystals were thicken to 24 nm after 1 h of heating at 125 °C. Samples annealed for 3 and 6 h had the same thickness of crystals determined by DSC – 27 nm. SAXS measurements of crystals' thickness, by applying a correlation function method, showed a similar tendency – an increase in the thickness of crystals with the annealing time, although the obtained values

Table 1
Crystalline structure of HDPE samples annealed at 125 °C as revealed by DSC and SAXS.

Annealing time [h]	Melting temperature [°C]	Enthalpy of melting [J/g]	Crystallinity [%]	Stem length [nm]	Lamellae thickness by DSC [nm]	Lamellae thickness by SAXS correlation function [nm]
0	133	191	66	24.5	20	16
1	135	216	75	29.4	24	21
3	136	224	78	33.0	27	24
6	136	233	81	33.0	27	25

were lower – initial 16 nm and final 25 nm. Control of thermal stability of polyethylene by Oxidation Induction Time method showed that the resistance of a polymer to thermooxidation does not change after annealing and is on the acceptable, yet not high, level of 3 min.

Mechanical properties of non-annealed and annealed dog-bone samples were determined during tensile drawing. The results are shown in Fig. 1. The engineering stress–strain curves in Fig. 1a represent drawing of samples annealed for 0, 1, 3 and 6 h and drawn at the same rate of $8.3 \times 10^{-4}\,s^{-1}$. Fig. 1b shows how the change in the strain rate influences mechanical properties of the sample annealed for 3 h. The strain rates of $8.3 \times 10^{-4}\,s^{-1}$, 6.7×10^{-5} and $2.5 \times 10^{-5}\,s^{-1}$ were applied. The annealing process modified the crystalline structure, as it was shown by DSC (see Table 1), and it is not surprising that mechanical properties of HDPE, particularly at yield, depend on the annealing procedure. Mechanical parameters at yield are presented in Table 2. The yield stress increases with the annealing time from 21.0 MPa for the initial specimen to 29.6 MPa for the sample annealed for the longest period of time. The yield strain shows the opposite tendency, i.e. it decreases with the annealing time from 18.0 to 12.2%. The observed changes in the yield behavior are characteristic of polymers in which crystallinity is increased.

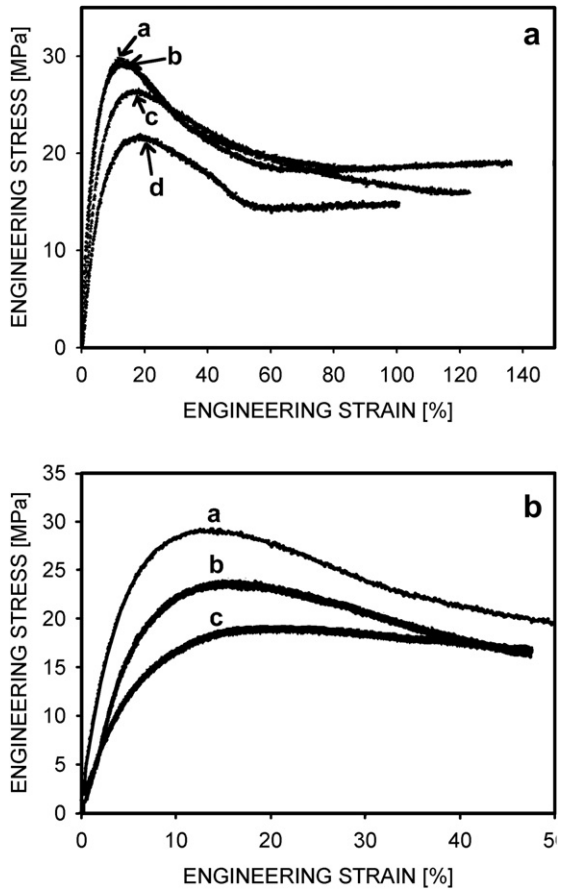

Fig. 1. Typical engineering stress-engineering strain dependence for HDPE. (1a) Different annealing times: a) 6 h, b) 3 h, c) 1 h, d) non-annealed; (1b) Different strain rates of samples annealed for 3 h at 125 °C: a) $8.3 \times 10^{-4}\,s^{-1}$, b) $6.7 \times 10^{-5}\,s^{-1}$, c) $2.5 \times 10^{-5}\,s^{-1}$.

The properties of HDPE at yield also depend on the deformation rate. A decrease in this rate results in a lower yield stress and a larger yield strain (Fig. 1b). Yield stress for polyethylene annealed 3 h is equal to 29.0 MPa when the strain rate is $8.3 \times 10^{-4}\,s^{-1}$, but only 19.0 MPa when the strain rate is $2.5 \times 10^{-5}\,s^{-1}$.

Our previous studies [11] demonstrated that cavitation in HDPE was not observed for the specimens cooled in iced water, for which the yield stress was 19 MPa. A limited number of cavities were detected in HDPE samples cooled in water (yield stress of 21 MPa) and intensive cavitation was observed for polyethylene samples solidified by slow cooling in air. The latter samples were characterized by the thickest crystals and the largest yield stress (26 MPa), which implies that either the yield stress or the thickness of crystals may be indicators of the lack or presence of cavitation during deformation. The stress threshold between these two possibilities for high density polyethylene seems to be around 21–22 MPa [11]. If the same rules applies here, then cavitation should be expected in all annealed samples tested at the standard speed ratio of 8.3×10^{-4}, but not in the initial material or in annealed polyethylene when a testing rate was very slow (Fig. 1b, curve c). Verification of this supposition is presented later.

It is known that plastic deformation of semicrystalline polymers is often strictly localized and that a neck is formed. In our samples the neck was visible when the engineering strain reached 30–40%. Local strains in the neck region were much larger than macroscopic engineering strains. Fig. 2 presents relations between the local strain, measured in the most deformed part of the neck, and the engineering strain.

The linear local strain-engineering strain dependence is observed when engineering strain is below 20%. For the larger values of engineering strain the localization of strains are visible in all of the studied samples, however its range depends on previous annealing of the material. The localization of strain is strongest for non-annealed samples. When the engineering strain for such a sample is 60%, i.e. equivalent to 0.6 in the local strain definition, then the local strain in the most deformed part is 4.5. The localization of strain decreases with the annealing time, however even after 6 h of annealing a neck is formed and local strains are much larger than macroscopic. There are two reasons for stronger

Table 2
Yield properties of HDPE annealed samples.

Annealing time [h]	Strain rate [s^{-1}]	Yield stress [MPa]	Yield strain [%]
0	8.3×10^{-4}	21.0	18.0
1		26.4	16.5
3		29.0	12.7
6		29.6	12.2
3	6.7×10^{-5}	23.8	16.0
3	2.5×10^{-5}	19.0	19.3

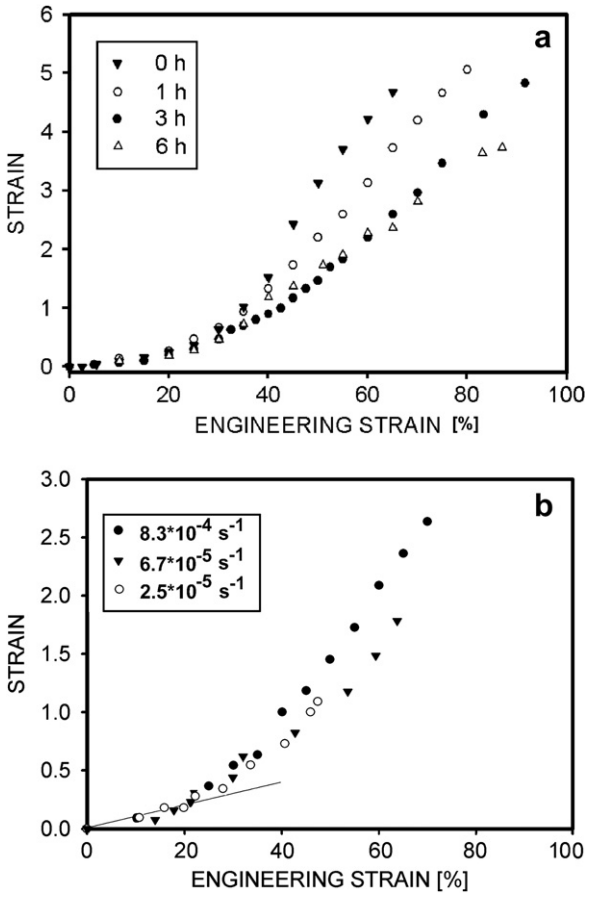

Fig. 2. Dependence of strain in the most deformed parts of HDPE samples as a function of engineering strain: (a) samples annealed at different times and stretched at the rate of 8.3×10^{-4} s^{-1}, (b) samples annealed for 3 h and stretched at different rates.

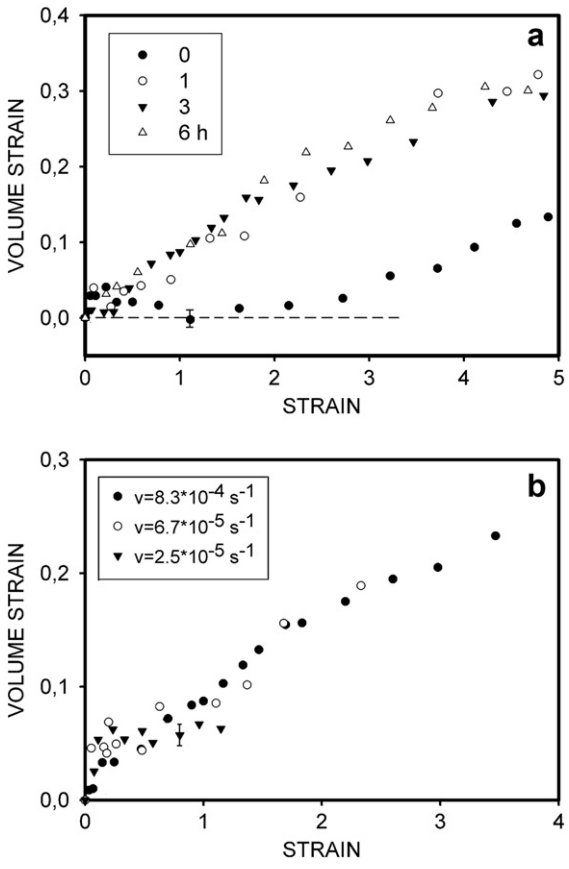

Fig. 3. Volume strain as a function of strain: (3a) different annealing times, (3b) different strain rates of samples annealed at 125 °C for 3 h. The error bar marked on the plot is representative of all data points.

deformation in non-annealed HDPE. The first one is connected with the crystalline phase, the second with the amorphous phase. Crystals in non-annealed polymers are thinner and more defected, therefore it is easier to initiate their plastic deformation, which leads to higher local deformation. Secondly, a non-annealed polymer sample contains more amorphous phase, which also favors deformation to larger extension [33,34].

Fig. 2b presents local-engineering strain dependence for samples annealed for 3 h and deformed at different rates. The linear dependence of engineering and local strains is preserved at the beginning of deformation. When larger strain is applied, an increase in the local strain is noted, accompanied by the formation of a neck. The curves in Fig. 2b also show that a decrease in the strain rate only slightly changes the localization of deformation.

Another aspect of the deformation process, observed for annealed samples, is whitening of the material in a necking zone. Submicrometer and micrometer-sized cavities formed during stretching are responsible for whitening. The whitening of polyethylene was noticed shortly beyond the yield point, i.e. before necking could be identified. Non-annealed specimens do not change their transparency with deformation, i.e. whitening does not occur in the material. Similarly, samples annealed for 3 h were still partially transparent if the strain rate was low, i.e. 2.5×10^{-5} s^{-1}.

Non-uniform strain distribution observed after yielding may be associated with local changes in volume, which can be measured by a video technique for the most deformed part of the gauge of the sample. These changes are presented in Fig. 3 in the form of a volume strain function. There is a significant difference in the shape of curves between non-annealed and annealed samples. In non-annealed HDPE a slight, 2–3%, increase in volume is observed for the strains of 0.3–0.4. At larger strains the volume decreases and for the strains in the range 1–2.5 even negative values of volume strain are obtained. G'Sell [35,36] attributed negative volume strain to the volume compaction of the amorphous phase as a result of orientation. The second positive range of the volume strain is observed when strains exceed 3.5. However, even for the strains close to 5.0 the volume of the most deformed part of the sample is only 15% larger than the initial one.

The annealed samples exhibited different behavior of volume strain. The shapes of curves representing annealing times of 1, 3 or 6 h are similar, as it is seen in Fig. 3a. The volume strain of each of the annealed samples quickly increases to 0.04 and with a further increase in the engineering strain, the increase is approximately linear. The 25–30% increase in volume was recorded for the strains of 3–5.

An increase in volume by 30% is much more than can be accounted for as a result of the Poisson ratio differing from 0.5. A typical reason for such a volume increase is formation of voids inside the material, responsible for whitening observed in the annealed samples.

Fig. 3b presents changes in volume of the samples annealed for 3 h, deformed at selected strain rates. Surprisingly, decreasing the strain rate did not significantly influence the volume strain–strain dependence. Even for the strain rate of 2.5×10^{-5} s^{-1} a significant increase in volume is observed in the deformed sample. Deformation of the annealed polyethylene sample at a slower rate is not accompanied by whitening, however its volume increases similarly

as in the case of a higher strain rate. It may suggest that numerous voids are created, though their size is smaller, much below a micrometer range.

The small-angle scattering patterns of synchrotron X-ray radiation, measured *in situ*, during deformation of samples are presented in Fig. 4. The images are correlated with the engineering stress-engineering strain curves and with local strains, indicated by the numbers below images. The scattering patterns change significantly with deformation. In the case of the non-annealed sample (see Fig. 4a) initially one only observes scattering from periodic crystalline structure in the shape of a ring. The ring preserves its shape up to the yield point, however later at the local strain of 0.25 it flattens in the direction parallel to direction of drawing and elongates in the direction perpendicular to direction of drawing. It means that the long period of the structure increases in the direction of drawing and decreases in perpendicular direction during deformation. The scattering image representing the local strain of 0.5 has an additional, more intensive signal, localized near the center. It is interpreted as an effect of limited voiding. The shape and orientation of scattering from voids change with deformation. The voids are elongated perpendicular to the direction of deformation up to the local strain of 0.5 and parallel to the direction of deformation for the strains of 1.0 and more.

Fig. 4b illustrates deformation and SAXS scattering for HDPE sample annealed for 1 h. Annealing changes the crystalline structure and the yield strength, however, for the local strains below 0.25 scattering images are very similar to those discussed above. Scattering from cavities is first detected at the local strain of 0.25 and the signal becomes much stronger when the local strain is increased to 0.4–0.6. Again, cavities are elongated perpendicularly to the direction of deformation and their change in shape starts at the local strain of approx. 0.6. Apparently for each level of deformation X-ray scattering is much stronger than the scattering from a deformed non-annealed sample.

Significant scattering from voids is observed in samples annealed for 3 h during deformation (Fig. 4c). Scattering from voids elongated perpendicularly to the direction of drawing, significantly exceeding the intensity of scattering from the crystalline structure, is observed for the local strain of 0.12, i.e. shortly before yielding. The intensity rapidly increases at yielding and then less strongly during further deformation. Scattering streaks from voids change their orientation with further deformation. Initially voids are oriented perpendicularly to the direction of deformation. At the local strain close to 0.7 the scattering pattern becomes approximately circular, while for larger strains it becomes elongated perpendicularly to the direction of deformation. The change in shape of scattering pattern is usually interpreted as a change of the voids' elongation from perpendicular direction to the direction of deformation. The second possibility – healing of the existing relatively large voids and formation of new, oriented in the direction of deformation, seems to be less probable because of approximately constant total intensity of scattering during reorganization of structure. Scattering from HDPE specimen annealed for 3 h is much stronger than scattering from HDPE sample annealed for 1 h.

X-ray scattering from the sample annealed for 6 h is similar to the scattering observed for shorter, 3 h, annealing time, which agrees with the observation that mechanical properties (yield) and crystal thickness are only slightly larger for the samples annealed for 6 h as compared to those annealed for 3 h. The differences from the material annealed for 3 h are that the total scattering intensity is slightly larger and that the change in the orientation of voids occurs later, at the local strain of around 0.8–1.0.

The change in shape of voids occurs during the strain softening process, before reaching the plateau on the engineering stress–strain curve. Reorientation is later detected for samples with a longer annealing time.

The change in scattering intensity resulted from the formation of voids and their further evolution are illustrated in Fig. 5, where

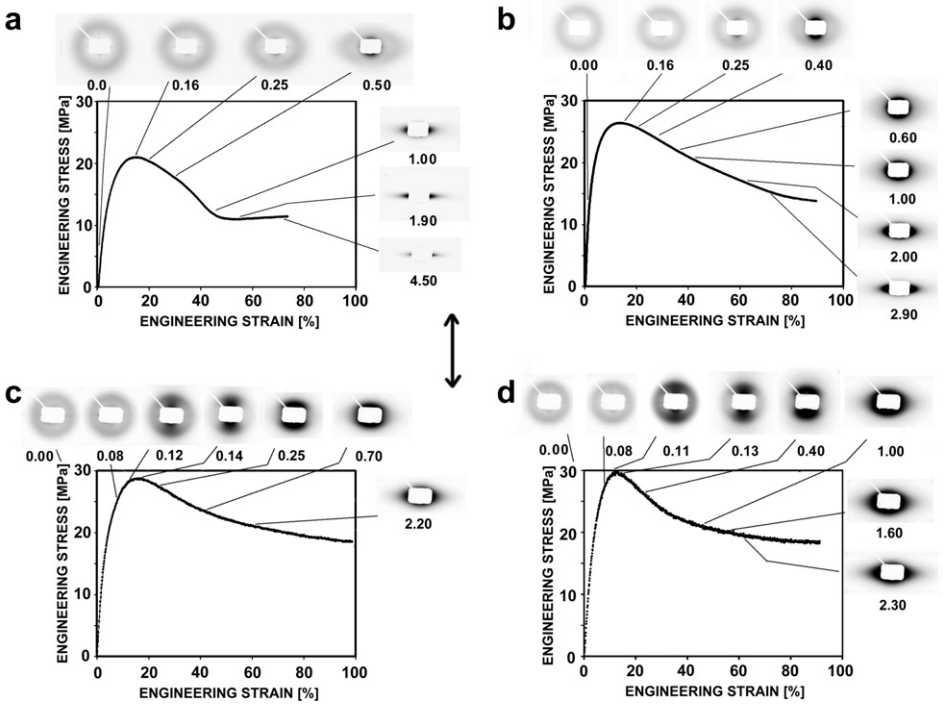

Fig. 4. SAXS scattering measured *in situ* during tensile drawing at the rate of 8.3×10^{-4} s^{-1}: a) non-annealed sample, b) sample annealed for 1 h, c) sample annealed for 3 h, d) sample annealed for 6 h. The numbers below SAXS patterns represent local strain in the sample at the moment of SAXS pattern recording. An arrow indicates the direction of deformation.

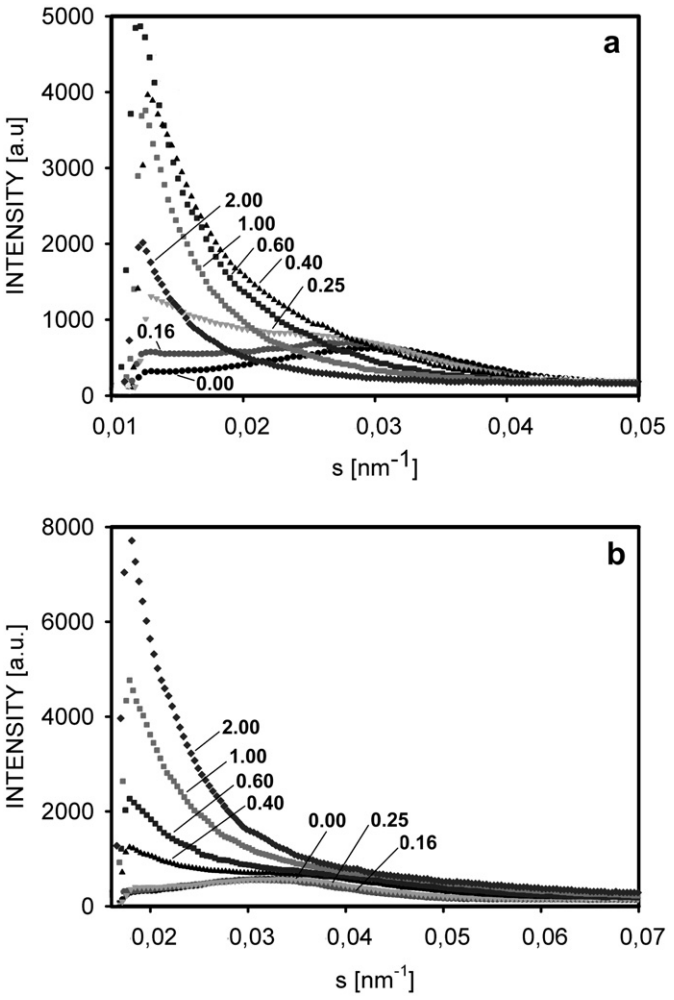

Fig. 5. The scattering intensities profiles vs. scattering vector, determined for the sample annealed for 1 h. The numbers near to symbols indicate local strain. The profiles were determined from the patterns in Fig. 4b along the vertical (a) and horizontal (b) directions.

the profiles of scattering intensity, I, vs. scattering vectors are presented for the sample annealed for 1 h. In Fig. 5 there are vertical and horizontal scans. For small deformation a maximum representing periodicity of lamellar structure is visible. The intensity begins to significantly increase in the vertical direction beyond yield (see Fig. 5a), i.e. when first cavities are formed. The increase is more rapid for the strains of 0.4 and 0.6, when the maximum intensity is reached. Meanwhile, there is an increase in intensity in the horizontal direction at the expense of signal in the vertical direction (Fig. 5b). The change of relation between intensities in the horizontal and vertical direction illustrates the change in shape of cavities with deformation.

Scattering patterns in Fig. 4 provide the source of information about the size of voids, which can be determined from a Guinier type plot using Yamashita's approach [29]. Vertical scan at a selected strain provided the basis for the analysis of the scattering profile and determination of the radii of gyration. We found that in all of the annealed samples two populations of voids can be separated. In deformed HDPE specimens annealed for 1 h voids with the radius of gyration $R_g = 18$ nm and 6 nm were observed. The samples annealed for 3 and 6 h also have two populations of voids characterized by the radii of gyration equal to 22 and 8 nm, respectively.

The knowledge of the radii of gyration is insufficient to determine the size of voids if their shape is unknown and if scattering objects are not randomly oriented. In our samples the shape of scattering patterns suggests that some orientation is present and that voids are elongated and ellipsoidal. Another observation is that for small strains scattering from cavities perpendicularly to deformation practically does not exist. It means that the size of cavities in the second direction is outside the SAXS detection range, i.e. they are either longer than 60 nm or shorter than approximately 1 nm.

The cavities change shape and later enlarge in the direction of drawing, which is visible as a progressive concentration of signal in the center of an image, near the beam stop. The sign of reshaping of cavities is noticed by scattering perpendicular to the direction of drawing that appears at the local strain of around 0.6 and increases with an increase in deformation.

Another subject of our studies by SAXS technique were samples annealed for 3 h and deformed with the decreasing strain rates of 6.7×10^{-5}, 2.5×10^{-5} s^{-1}. Measurements at these rates were not possible *in situ* (as illustrated in Fig. 4), as they were lower than the rate available in a tensile machine connected to synchrotron radiation facilities. Scattering patterns from HDPE sample deformed at slow rates are presented in Fig. 6a, b. These patterns were recorded from differently strained parts of samples after relaxation.

The images for HDPE deformed at the rate of 6.7×10^{-5} s^{-1} look similarly to those discussed previously for deformation at the rate of 8.3×10^{-4} s^{-1}. Intensive scattering from voids is observed. Further decrease in the strain rate to 2.5×10^{-5} s^{-1}, i.e. only to 0.15% of the initial gauge length per minute, effectively reduced the scattering intensity. The voids were not detected neither around yield, nor for the local strain of 1.1 in such slowly deformed samples after being released from clamps (Fig. 6b).

The conclusion from Figs. 3b and 6b is that voids are formed during deformation but they are healed upon unloading the sample. To clearly illustrate this phenomena the following experiment was conducted – the sample was drawn at the strain rate of 8.3×10^{-4} s^{-1} and the SAXS pattern recorded during straining at the strain of 0.15. Next, the sample was relaxed by releasing from grips and the SAXS pattern was recorded after a 10 min waiting period. Fig. 6c illustrates that although cavities were formed during drawing, no cavities were detected by SAXS after relaxation (Fig. 6c, II). It must be mentioned

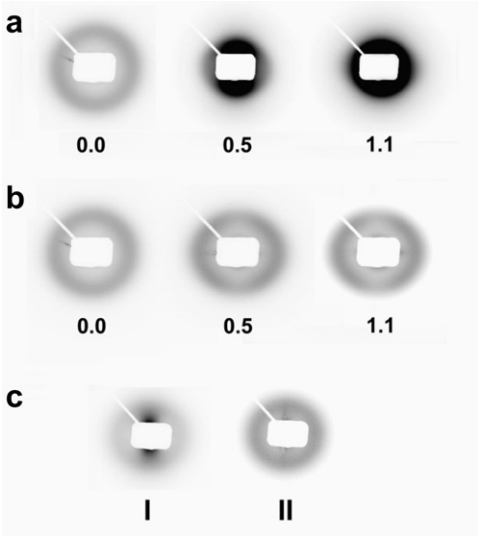

Fig. 6. Scattering patterns from HDPE samples annealed 3 h and deformed at the rate of 6.7×10^{-5} s^{-1} (a), 2.5×10^{-5} s^{-1} (b) and 8.3×10^{-4} s^{-1} (c). The numbers below images represent local strain. The samples were deformed in the vertical direction. SAXS patterns of samples in (a) and (b) were recorded after relaxation. SAXS pattern of the sample in (c) was recorded under stress (I) when the strain was 0.15 and after relaxation (II).

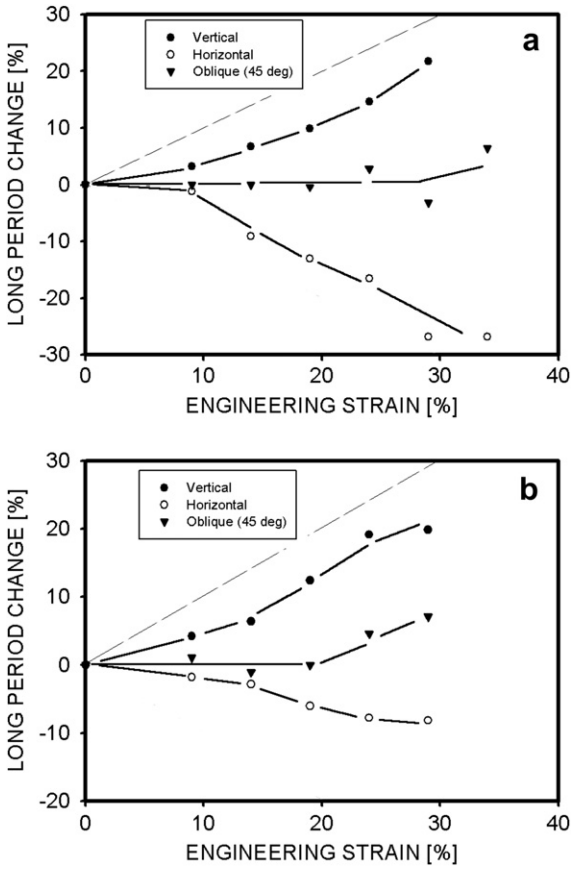

Fig. 7. Change in the long period for non-annealed (a) and annealed for 1 h (b) HDPE samples during deformation at the strain rate of 8.3×10^{-4} s^{-1}, determined from SAXS patterns *in situ* recorded in vertical (●), horizontal (○) 45° directions (▼).

that such healing of voids is only possible for a relatively low strain and a low strain rate. Another interesting observation has been made while comparing the parts of SAXS scattering from the crystalline structure. In Fig. 6b orientation of lamellae is observed, although cavities disappeared, while in Fig. 6c lamellar orientation and cavities apparently are not present.

If cavities are present in a polymer, they are formed inside the amorphous phase between the existing crystalline elements. It means that the cavitation process and the development of the cavities' shape and size depend on the morphological changes of the surrounding polymeric matrix. These changes may be studied by analyzing the long period from SAXS experiment and by collecting data from wide-angle X-ray diffraction.

In SAXS patterns of a cavitating polymer scattering from cavities dominates and overlaps scattering from the periodic crystalline structures – lamellar stacks. In our samples the analysis of the change in the long period with deformation was only possible for non-annealed specimens and HDPE specimens annealed for 1 h. For this purpose patterns in Fig. 4a, b were used. The results are presented in Fig. 7 for three directions of scanning: vertical, horizontal and oblique at 45°. A vertical profile is taken in the direction of deformation and represents lamellar stacks in which surfaces of lamellae are perpendicular to direction of deformation. Usually, if a polymer has a spherulitic morphology, those crystals are present in the equatorial zones of spherulites. Horizontal scattering originates from lamellar stacks in which surfaces of lamellae are parallel to the direction of deformation. The presence of such lamellae is expected in the polar regions of spherulites. The synchrotron measurements provided the following values of long periods for non-deformed samples: 25.4 nm for non-annealed HDPE and 28.2 nm for polymer annealed for 1 h. The increase in the long period is observed on annealing of several polymers and it is plausibly explained by the mechanism of crystal thickening and sliding diffusion (e.g. [37]).

Fig. 7 shows that the values of long period change significantly with deformation and these changes depend on the direction of measurements. In the vertical direction the long period increases with deformation for both non-annealed and annealed specimens. The opposite tendency is visible in the horizontal direction, where the characteristic lamellar stack distance decreases with deformation. Such results are not surprising because lamellar stacks are strained in the equatorial regions and compressed in the polar regions of spherulites [1,5,8,14,16]. It is interesting to note that the increase in the long period in the vertical direction is smaller than the increase in the engineering strain. A similar tendency has recently been described by Humbert et al. [38].

The long period for the polar region of lamellae in non-annealed samples decreases to 18.5 nm at the strain of 30–35%. The thickness

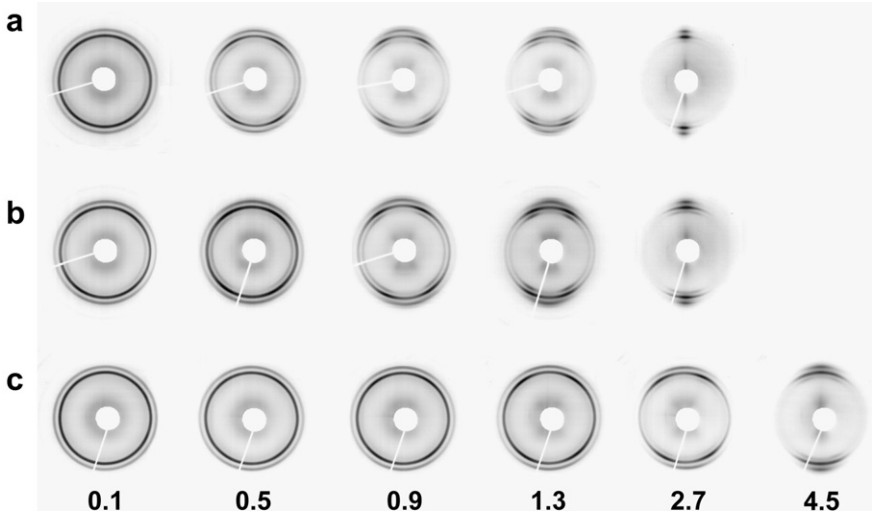

Fig. 8. WAXS patterns from HDPE samples: a) non-annealed sample, deformed and kept at the fixed strain, b) sample annealed for 3 h, deformed and kept at the fixed strain, c) sample annealed for 3 h, deformed and relaxed with free ends. The numbers indicate local strain. The direction of deformation – horizontal.

of crystalline layers in the non-deformed sample, calculated from the degree of crystallinity (Table 1) and the initial long period, is 17 nm. It means that the amorphous material between crystals is strongly compressed and that also crystals become thinner as a result of crystallographic slips. Similar calculations for samples annealed for 1 h, give the values of initial thickness of crystals of 21.1 nm and the final long period of 25.9 nm. It means that the thickness of amorphous phase also significantly decreases during deformation, however the decrease is smaller than in the case of non-annealed polypropylene.

In the parts of spherulites oriented at 45° it is assumed that interlamellar shear occurs at the beginning of plastic deformation, without a change in the distance between lamellae. It agrees with the observation that the long period is preserved up to the engineering strain of 20%. For larger strains the distance between crystals in these positions increases, which is probably the result of fragmentation of crystals.

Fig. 8 presents WAXS patterns obtained from non-annealed and annealed specimens, deformed to selected strains. The measurements were performed after drawing, but the samples remained fixed in a special frame preserving the strain state. The sample annealed for 3 h was also analyzed after relaxation. The numbers in Fig. 8 indicate the local strain reached during drawing.

The two circles which appear in WAXS patterns for the unoriented material and strained to 0.1 (Fig. 8a, b) are associated with diffraction from 110 (inner circle) and 200 (outer circle) lattice planes. In samples under the preserved strain, a third ring appears inside the (110) ring indexed as (001) of monoclinic form. This form is a result of martensitic transformation from orthorhombic form under stress. The monoclinic form is not visible in the pattern at such a strain if the sample is relaxed with free ends (see Fig. 8c).

A four-point pattern of (110) ring is formed after yielding. Also a decrease in the intensity of diffraction from (200) plane on meridian and an increase on the equator is observed.

The four-point (110) pattern is usually formed by the (100) chain slip of crystals and is associated with tilting and the onset of lamellar fragmentation [8,39,40]. At the larger strain of 0.9 another four-point pattern is formed by diffraction on crystals of monoclinic form.

The monoclinic form is not observed in the relaxed samples, even at the strain of 1.3. The effects of plastic deformation represented by changes of diffraction rings are visible in the relaxed polymer for local strains larger than in the same material under stress.

The transition of (110) a four-point pattern into two arcs is noted for the strain in the range 1.3–2.7. At this strain the concentration of (200) reflections near the equator is also visible. Monoclinic phase with its (001) diffraction ring is detected in deformed and relaxed samples at a strain approaching 2.7.

One can draw two conclusions from WAXS observations: there is no difference in diffraction patterns between non-annealed and annealed samples and much of the deformation including martensitic transformation is reversible, even if the sample is strained beyond the yield. WAXS patterns obtained from the deformed sample released from grips might not be representative of the morphological changes under strain.

4. Conclusions

Annealing of semicrystalline polymers at elevated temperature changes the thickness of crystals, crystallinity and perfection of crystals as well as the ability of polyethylene to cavitate. By annealing we were able to increase the crystallinity from 66 to 81% and lamellar thickness, as determined from DSC thermograms, from 20 to 27 nm. This resulted in an increase in the resistance of crystals to plastic deformation. The amorphous phase became thinner, the density of entanglements increased as the same number of entanglements are concentrated in smaller volume and the chains are strained, because their fragments were pulled from the amorphous phase and incorporated within crystals. It follows that annealed polyethylene samples exhibit higher yield stress due to thicker crystals, while the amorphous phase becomes more fragile and vulnerable to cavitation.

An X-ray scattering experiment confirmed that voids are not generated at yield in non-annealed samples, however even short annealing favors cavitation near yielding. The intensity of cavitation depends on the momentary strain and on the time of annealing. The voids detected by SAXS are in a nanometer range, but whitening indicates that also larger, micrometer size voids are formed during drawing. The shape of cavities evolves with an increase in strain – the change in the orientation of scattering from voids is visible during strain softening when a neck is formed. The analysis of SAXS patterns has also demonstrated that in non-annealed samples, at the strains of 0.5 and more, a limited number of voids are formed. Those voids are generated during the final transformation of fragmented lamellae into fibrils. That is also confirmed by the increase in volume (Fig. 3a).

Cavitation is a massive phenomenon in annealed HDPE specimens, which is visible as an increase in volume of the sample. The significant and approximately linear increase in the volume is observed, beginning with yielding. The volume of a sample increases up to 30% for a higher strain. There is no doubt that cavitation is responsible for the volume increase, because non-annealed and non-cavitating polyethylene preserves its volume up to large strains.

Plastic deformation of crystals at a slower deformation rate is easier as it is a rate-controlled phenomenon. With a slower deformation rate crystals are easily deformed and cavitation is not initiated. At very slow tensile drawing cavities may be not stable and heal. At the slowest straining rate of $2.5 \times 10^{-5}\ s^{-1}$ voids were detected only in the stressed samples. Martensitic transformation from orthorhombic form into monoclinic form of PE occurs under stress and is reversible when the sample is unloaded.

Acknowledgments

We wish to express thanks to the Hamburg Synchrotron Radiation Laboratory (HASYLAB) for the beam time granted within the project I 20070061 EC. Also the grant N N508 468834 from the Polish Ministry of Science and Higher Education is acknowledged for the financial support of the work.

References

[1] Galeski A. Prog Polym Sci 2003;28(12):1643–99.
[2] Brown EN, Dattelbaum DM, Brown DW, Rae PJ, Clausen B. Polymer 2007;48(9):2531–6.
[3] Duffo P, Monasse B, Haudin JM, G'Sell C, Dahoun A. J Mater Sci 1995;30(3):701–11.
[4] Li JX, Cheung WL. Polymer 1999;40(8):2089–102.
[5] Butler MF, Donald AM, Ryan AJ. Polymer 1997;38(22):5521–38.
[6] Castagnet S, Girault S, Gacougnolle JL, Dang P. Polymer 2000;41(21):7523–30.
[7] Nathani H, Dasari A, Misra RDK. Acta Mater 2004;52(11):3217–27.
[8] Butler MF, Donald AM, Ryan AJ. Polymer 1998;39(1):39–52.
[9] Gencur SJ, Rimnac CM, Kurtz SM. Biomaterials 2003;24(22):3947–54.
[10] Pawlak A, Galeski A. Macromolecules 2005;38(23):9688–97.
[11] Pawlak A. Polymer 2007;48(5):1397–409.
[12] Pawlak A, Galeski A. J Polym Sci Part B Polym Phys 2010;48(12):1271–80.
[13] Pawlak A, Galeski A. Macromolecules 2008;41(8):2839–51.
[14] Addiego F, Dahoun A, G'Sell C, Hiver JM. Polymer 2006;47(12):4387–99.
[15] Schneider K, Trabelsi S, Zafeiropoulos NE, Davies R, Riekel C, Stamm M. Macromol Symp 2006;236:241–8.
[16] Butler MF, Donald AM, Bras W, Mant GR, Derbyshire GE, Ryan AJ. Macromolecules 1995;28(19):6383–93.
[17] Butler MF, Donald AM, Ryan AJ. Polymer 1998;39(4):781–92.
[18] G'Sell C, Hiver JM, Dahoun A. Int J Solids Struct 2002;39(13):3857–72.

[19] Lazzeri A, Thio YS, Cohen RE. J Appl Polym Sci 2004;91(2):925–35.
[20] Stribeck N, Nochel U, Funari SS, Schubert T, Timmann A. Macromol Chem Phys 2008;209:1992–2002.
[21] Stribeck N, Nochel U, Funari SS, Schubert T. J Pol Sci Part B Polym Phys 2008;46(7):721–6.
[22] Wu J, Schultz JM, Yeh F, Hsiao BS, Chu B. Macromolecules 2000;33(5):1765–77.
[23] Murthy NS, Bednarczyk C, Moore RAF, Grubb DT. J Polym Sci Part B Polym Phys 1996;34(5):821–35.
[24] Jiang Z, Tang Y, Men Y, Enderle HF, Lilge D, Roth SV, et al. Macromolecules 2007;40(20):7263–9.
[25] Men Y, Rieger J, Homeyer J. Macromolecules 2004;37(25):9481–8.
[26] Hughes DJ, Mahendrasingam A, Oatway WB, Heeley EL, Martin C, Fuller W. Polymer 1997;38(26):6427–30.
[27] Strobl GR, Schneider M. J Polym Sci Polym Phys Ed 1980;18(6):1343–59.
[28] Goderis B, Reynaers H, Koch MHJ, Mathot VBF. J Polym Sci Part B Polym Phys 1999;37(14):1715–38.
[29] Yamashita T, Nabeshima Y. Polymer 2000;41(16):6067–79.
[30] Hoffman JD. Polymer 1982;23(5):656–70.
[31] Patel D, Bassett DC. Polymer 2002;43(13):3795–802.
[32] Brown EN, Willms RB, Gray III GT, Rae PJ, Cady CM, Vecchio KS, et al. Exp Mech 2007;47(3):381–93.
[33] Séguéla R. Macromol Mater Eng 2007;292:235–44.
[34] Humbert S, Lame O, Vigier G. Polymer 2009;50(15):3755–61.
[35] Quatravaux T, Elkoun S, G'Sell C, Cangemi L, Meimon Y. J Polym Sci Part B Polym Phys 2002;40(22):2516–22.
[36] Cangemi L, Elkoun S, G'Sell C, Meimon Y. J Appl Polym Sci 2004;91(3):1784–91.
[37] Hikosaka M, Watanabe K, Okada K, Yamazaki S. Adv Polym Sci 2005;191:137–86.
[38] Humbert S, Lame O, Chenal JM, Rochas C, Vigier G. J Pol Sci Part B Polym Phys 2010;48(13):1535–42.
[39] Hiss R, Hobeika S, Lynn C, Strobl G. Macromolecules 1999;32(13):4390–403.
[40] Galeski A, Bartczak Z, Argon AS, Cohen RE. Macromolecules 1992;25 (21):5705–18.